inter.noise
21-24 AUGUST
SCOTTISH EVENT CAMPUS
GLASGOW 2022

An experimental investigation into the influence of installed chevron jet flows on wall-pressure fluctuations

Edoardo Carbini[1], Stefano Meloni[2] and Roberto Camussi[3]
Department of Engineering, University of Roma Tre
Rome 00146 RM, Italy

Jack Lawrence[4] and Anderson Proença[5]
Institute of Sound Vibration Research, University of Southampton
Southampton SO17 1BJ, UK

ABSTRACT

Jet-surface interaction represents a significant community noise problem for the installation of modern ultra-high bypass ratio turbofan engines. The use of chevron nozzles is known to reduce low-frequency jet mixing noise by increasing the mixing rate close to the nozzle. It is currently unknown, however, to what extent such a nozzle lip treatment affects the Kelvin-Helmholtz instability, generated in the vicinity of the wing, which will modify the source of jet-surface interaction noise. To clarify the physics of the jet-surface interaction noise source, an extensive experimental investigation was conducted using the Flight Jet Rig in the anechoic chamber of the Doak Laboratory, at the University of Southampton. Various measurements were carried out on a round and a chevron single stream, unheated subsonic jet, both in an isolated configuration and installed beneath a 2D NACA4415 airfoil "wing". The wall-pressure field on the wing surface was investigated using a pair of miniature wall-pressure transducers and a set of ultra-thin precision microphones. These sensors were flush-mounted in both the stream-wise and span-wise directions on the pressure side of the wing and the unsteady wall-pressure data were analysed in the time and frequency domains. The far-field noise results show significant broadband noise reduction by the chevron jet. This is further evidenced by a reduction in the span-wise correlation length along the wing trailing edge over a wide range of frequencies. Significant reduction of the tonal trapped wave energy is also observed.

1. INTRODUCTION

In recent years, the aviation authorities have strengthened noise regulations for aircraft at airports forcing aircraft manufacturers to invest resources in aeroacoustic research. In particular, these stringent noise regulations make jet-surface interaction (JSI) a significant community noise problem

[1]edo.carbini@stud.uniroma3.it

[2]stefano.meloni@uniroma3.it

[3]roberto.camussi@uniroma3.it

[4]j.lawrence@soton.ac.uk

[5]a.proenca@cranfield.ac.uk

hindering the installation of modern ultra-high bypass ratio (UHBR) turbofan engines. In recent decades, research has focused on decreasing the jet mixing (JM) noise, which is a significant contribution to engine acoustic signatures at take-off and plays a key role in the sideline certification position [1]. Historically, chevrons have been introduced to reduce JM noise by increasing the mixing rate in the jet shear layer, generating less low-frequency energy at the expense of more high-frequency energy, which is better attenuated by the atmosphere [2]. What is currently unclear is to what extent any modifications to the flow-field impact the Kelvin-Helmholtz instability generation responsible for the JSI noise source contribution in future closely coupled UHBR engine-wing aircraft.

The behaviour of chevrons is well represented in the literature. Parametric studies on uniformly distributed chevron nozzles have been carried out, investigating the effects on far-field noise and azimuthal modes. Several authors have observed a strong dependence on the chevron count and angle of flow penetration [3,4]. Other relevant studies have been carried out on azimuthally varying chevron designs for typical take-off conditions [5–8]. The above-mentioned works show a substantial noise reduction (e.g. up to 3 dB) when there is an asymmetric chevron distribution in both the isolated and installed situations. The wall-pressure fluctuations induced by the jet have been investigated in model-scaled experiments [9–11]. In particular, single-point and two-point statistics were analysed for both a simpler jet-plate configuration [9] and a more complex jet-wing configuration [10].

This paper focuses on the physics of the noise reduction mechanism behind a uniformly distributed installed chevron nozzle. First, the far-field acoustic pressure field is investigated experimentally using two model-scale single-stream jets: a baseline axisymmetric jet and a chevron jet with 16 chevrons and a 9° penetration angle installed beneath a NACA4415 wing. Wall-pressure fluctuation data were recorded in both the stream-wise and span-wise directions using several flush-mounted transducers on the pressure side of the wing. Far-field acoustic data were acquired synchronously with wall-pressure measurements using a linear flyover microphone array. The data are analysed in both the time and frequency domains to characterise the pertinent physical mechanisms.

The paper is organized as follows: Section 2 introduces the experimental facility and methodology. In Section 3, results for the far-field noise are analysed to define the effects of chevrons in both the isolated and installed configurations. Next, the surface TE span-wise coherence is presented as a function of wing position. Finally, a discussion regarding the span-wise correlation length is given before the main conclusions are presented.

2. EXPERIMENTAL SETUP

A model-scale static jet experiment was undertaken using the Flight Jet Rig (FJR) in the Doak Laboratory within the Institute of Sound and Vibration Research (ISVR), at the University of Southampton. The Doak Laboratory is a small-scale anechoic chamber, fully anechoic down to 400Hz. The facility has dimensions approximately equal to 15m-long, 7m-wide and 5m-high. A high-pressure compressor-reservoir system supplies the air jet, which, for this test, was operated at a fixed jet acoustic Mach number, $M_j = 0.6$. The jet conditions were determined from real-time measurements of total temperature and total pressure. The jet exit velocity was kept within a tolerance of ±5 m/s. In addition, ambient temperature, relative humidity and ambient pressure were recorded within the laboratory to compute the acoustic Mach number and to ensure repeatability across previous tests with different climactic conditions.

The test was divided into two configurations: isolated and installed jet. Two different 3D-printed 50mm-diameter nozzles were used for each case: a baseline round "R50" nozzle and a chevron "R50-CN-N16-A09" nozzle with 16 chevrons and a 9° flow penetration angle, see Figure 1.

A NACA4415 wing profile, with a 150mm chord and 600mm span, was installed at different positions relative to the nozzle exit. Two parameters define the position of the wing, H/D and L/D, where H is the vertical distance between the jet centreline axis and the wing trailing edge, L is the stream-wise

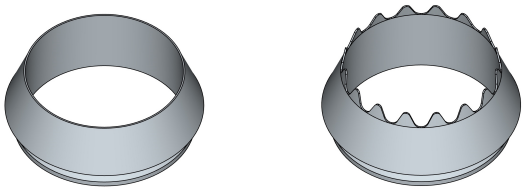

(a) (b)

Figure 1: A sketch of the two nozzle exit configurations: a) baseline round nozzle, R50; b) 16-chevron nozzle, R50-CN-N16-A09.

distance between the jet exit plane and the wing TE, and D is the nozzle exit internal diameter. The values of these parameters are $H/D = 0.6, 1$ and $L/D = 2, 3$, see Figure 3. The wing was secured at an angle of attack of 4° using a support structure.

The far-field acoustic data was acquired with a fixed linear "flyover" array (at azimuthal angle $\varphi = 0°$) consisting of twelve 1/4" B&K Type 4939 capsules, each conditioned with G.R.A.S. Type 26AN preamplifiers. Each microphone was mounted within a rigid tube and attached equally spaced to a truss on the chamber ceiling 2m radially from the x-axis. The resulting polar angles were $45° \leq \vartheta_j \leq 140°$, where ϑ_j is defined relative to the jet axis. Each microphone was oriented at 0° incidence to the jet axis.

The wall-pressure measurements were performed using a pair of Kulite LQ-062 Ultraminiature Thin Line Pressure Transducers with a sensing diameter of 1.6mm and five G.R.A.S. 48LA UTP microphones with a sensing diameter of 5mm. All sensors were housed in dedicated 3D-printed holders within a cartridge installed on the wing pressure surface. Figure 2 shows the arrangement of the transducers on the cartridge. Transducers M to R are UTPs and S and T are Kulites. T, O, N and M are on the right side of the cartridge at a distance of 5, 20, 40 and 85mm from S, respectively. Q and R are on the left side at a distance of 10 and 85mm from S, respectively. P was the only transducer in the stream-wise direction, at a distance of 15mm from S. The transducers in the span-wise direction (i.e., M, N, O, Q, R, S and T) were used to compute the coherence relative to the reference sensor, S, located on the axis of the jet.

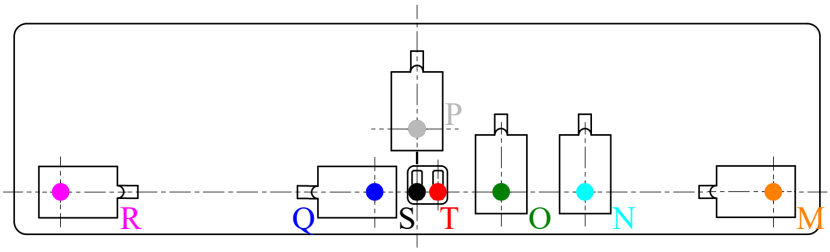

Figure 2: Sketch of the wing sensor cartridge.

The microphone unsteady voltage data was digitised using a National Instruments PXIe-4497 Dynamic Signal Analyser at a sample rate of 200 kHz with 24-bit resolution.

The far-field signals were acquired for 10 seconds, 20 Hz high-pass filtered and then amplified using six G.R.A.S. Type 12AQ amplifiers. The time signals were corrected for amplifier gain and capsule calibration sensitivity and then transformed to the frequency domain using a Hamming window-averaged Fast Fourier Transform following Welch's overlapped segment-averaging spectral estimation method [12]. To obtain data above 10kHz, all microphone capsule protection grids were removed. The spectral data plotted herein is reported as a sound pressure level (ref. 20μPa) with 100Hz frequency band resolution. Finally, a 1m distance correction (based on spherical spreading)

and an atmospheric absorption correction were also applied to the data [13, 14]. The wall-pressure data were acquired synchronously with the far-field acoustic data for 10 seconds at a sampling frequency of 200kHz. The Kulite transducers were controlled via a signal conditioner (KSC-2) where an excitation voltage of 5V, a pregain of 128 and a cut-off filter of 100kHz were imposed. The UTP transducers were amplified with a 16-channel B&K Type 2694 CCLD conditioning amplifier.

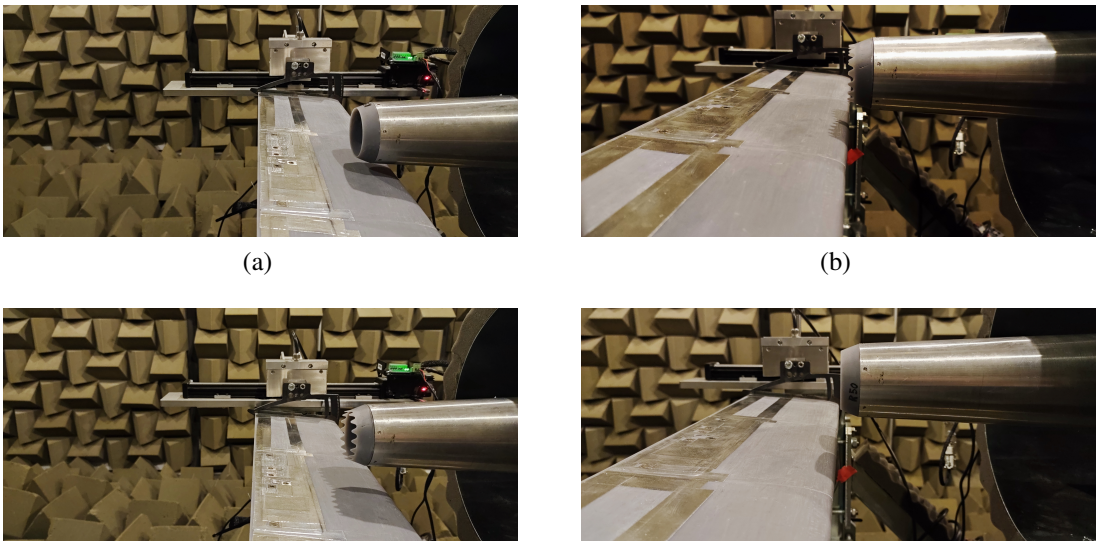

(a) (b) (c) (d)

Figure 3: Pictures of the different installed jet setups: a) $H/D = 0.6$, $L/D = 2$; b) $H/D = 0.6$, $L/D = 3$; c) $H/D = 1$, $L/D = 2$; d) $H/D = 1$, $L/D = 3$.

3. RESULTS

Firstly, the far-field data are analysed to check the JM noise effects produced by the chevrons in the isolated jet configuration. Next, the impact of the chevrons on the JSI noise, when the jet is installed beneath the wing, is studied. Finally, wall pressure fluctuations are analysed to better understand the physics of the JSI noise source mechanism.
The unsteady pressure measurements were analysed in the frequency domain and the acoustic data are plotted as sound pressure levels, evaluated according to the following equation:

$$\mathrm{SPL} = 10 \log \frac{P_{xx}\, \Delta f_{ref}}{p_{ref}^2}, \tag{1}$$

where P_{xx} is the auto power spectral density computed via Welch's method, Δf_{ref} is the frequency bandwidth, set at 100Hz, and p_{ref} is the acoustic reference pressure, equal to 20μPa.
Figure 4 shows the spectra obtained from the far-field microphone positioned at $\vartheta = 90°$ and $\varphi = 0°$ for both nozzles in the isolated jet configuration. The jet acoustic Mach number was fixed at $M_j = 0.6$. Looking at Figure 4, a typical chevron jet trend emerges: an noise reduction at low and mid frequencies and a penalty at high frequencies beyond a cross-over frequency. In Figure 4b these features are reported in terms of ΔSPL, defined as:

$$\Delta\mathrm{SPL} = \mathrm{SPL}_{\mathrm{CN}} - \mathrm{SPL}_{\mathrm{R50}}. \tag{2}$$

When the both jets are installed close to the wing surface, the noise observed in the far-field changes dramatically. Figure 5a clearly illustrates this effect compared to the isolated case. As expected, a large low-frequency noise increase is observed for the installed-jet case and with a strong

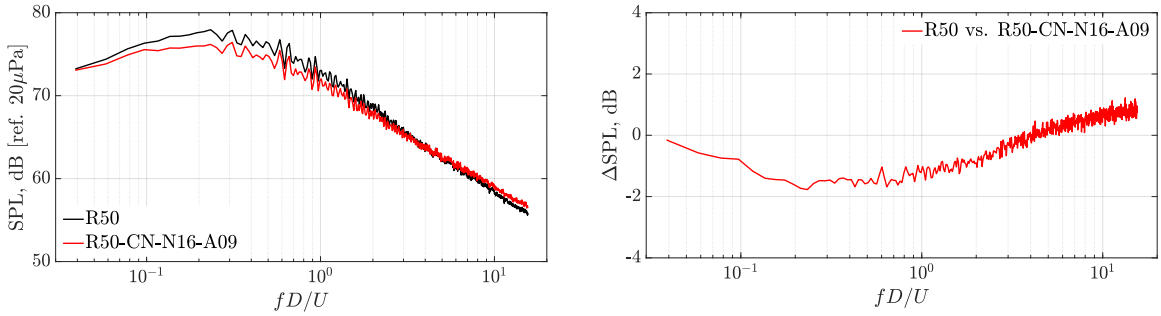

(a) (b)

Figure 4: Far-field autospectra of the isolated baseline and chevron jets; [$\vartheta = 90°$, $\varphi = 0°$, $M_j = 0.6$].

dependence on radial distance between jet and wing. Additionally, tonal components are observed in the spectra at wing configurations particularly close to the jet axis ($H/D = 0.6$), green and cyan lines. These tonal features are likely related to the trapped waves that exist within the jet [15], which are scattered to the far-field by the wing TE.

At high frequencies, the presence of the wing produces a quasi-constant increase in energy content due to reflected JM noise. This energy is visible because the ceiling far-field flyover microphone array is positioned above the wing, in an unshielded position (i.e., $\varphi = 0°$). Figure 5b shows the effects the chevrons have on the installed jet in terms of ΔSPL. From Figure 5b, two main chevron effects are observed: (1) a significant low-frequency broadband noise reduction is introduced (up to 3dB, depending on the particular jet-wing configuration), and (2) the tonal energy is completely eliminated. Both of these effects are more pronounced the more aggressively the jet is coupled to the wing.

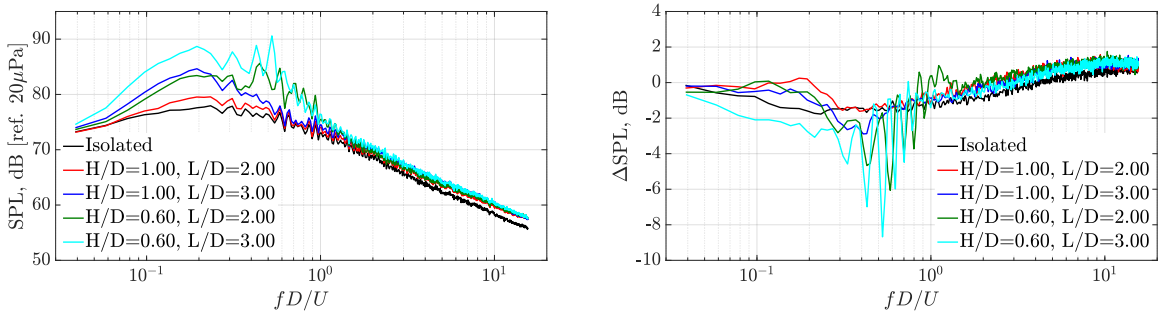

(a) (b)

Figure 5: Far-field acoustic spectra [$\vartheta = 90°$, $\varphi = 0°$, $M_j = 0.6$]. a) Sound pressure level of the installed R50 nozzle at varying jet-wing position; b) Delta sound pressure level between the chevron and baseline jets at varying jet-wing position.

To better understand what was observed in the far-field, the signal coherence between the microphones placed along the span of the wing near the TE were analysed. The squared coherence function has been calculated using the following expression:

$$\gamma^2(\xi, \eta, \omega) = \frac{|P_{xy}(\xi, \eta, \omega)|^2}{P_{xx}(\omega)\, P_{yy}(\omega)}, \tag{3}$$

where P_{xy} is the cross power spectral density between two different transducer signals x and y, while P_{xx} and P_{yy} are the auto power spectral densities of x and y, respectively.

Figure 6 shows a comparison of the span-wise coherence values for the two nozzles at $M_j = 0.6$. The solid lines refer to the baseline nozzle (R50) and the dotted lines refer to the chevron nozzle (CN). The colours in the plots refer to the coherence between a particular microphone, see Figure 2, and the reference transducer S. The authors have chosen to report the data at a single axial wing location, $L/D = 2$, which is most representative of future UHBR aircraft. Figure 6a shows the coherence at $H/D = 1$. Firstly, as expected, the coherence is observed to decrease with increasing span-wise distance. The orange and fuchsia lines are related to the two transducers farthest from the jet axis (M, R). Their shapes closely match the far-field spectra. The effect of the chevrons appears to be small for this configuration. Figure 6b, however, shows the more aggressively coupled configuration, at $H/D = 0.6$. For display clarity, only data from transducers T and Q (referenced to S) are shown. Both a significant broadband reduction (by as much as 30%) and tonal noise reduction can be seen clearly.

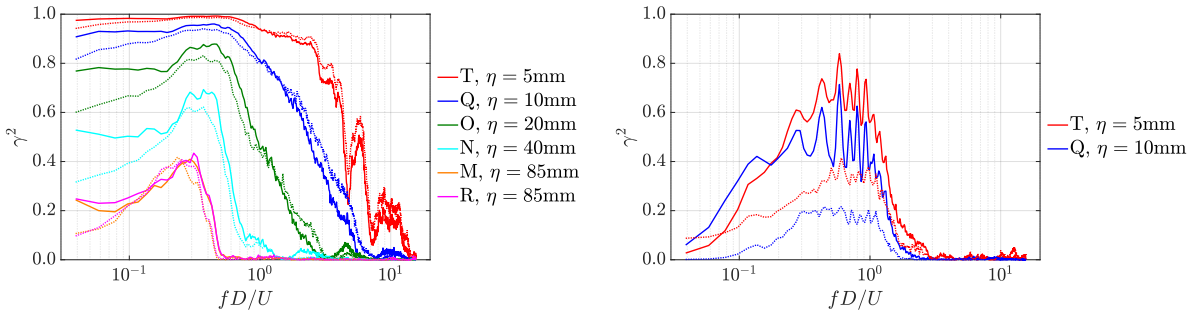

Figure 6: Surface TE span-wise coherence [solid lines refer to the R50 nozzle, dotted lines refer to CN nozzle]. $M_j = 0.6$. a) $H/D = 1$, $L/D = 2$; b) $H/D = 0.6$, $L/D = 2$

Finally, the span-wise correlation lengths were also calculated using:

$$\Lambda(\omega) = \int_0^\infty \gamma^2(\eta, \omega)\, d\eta \tag{4}$$

where η is the distance between transducers in span-wise direction. The correlation length is non-dimensionalised with the jet diameter D and the results are presented in Figure 7. As already evidenced, the jet-wing distance is observed to play a key role. It can be seen that, at $H/D = 1$, the chevrons do have a small effect on the lowest frequency energy. At $H/D = 0.6$, the chevrons are observed to roughly halve the span-wise correlation length over the frequency range of interest.

4. CONCLUSIONS

An experimental investigation detailing the effects of nozzle chevrons on the generation of both far and wall pressure fields of a model-scale installed jet has been presented. The study included far-field noise and wall-pressure fluctuation analyses under static ambient flow conditions at a fixed jet acoustic Mach number, $M_j = 0.6$. The experimental setup consisted of two nozzles, one round axisymmetric and the other with 16 chevrons with a flow penetration angle of 9°. The nozzles were mounted beneath a 2D NACA4415 wing at four nozzle-wing locations. The wing was designed to accommodate a sensor cartridge to position several flush-mounted transducers on the pressure surface. The far-field noise was analysed using a fixed linear 12-microphone flyover array. For the isolated

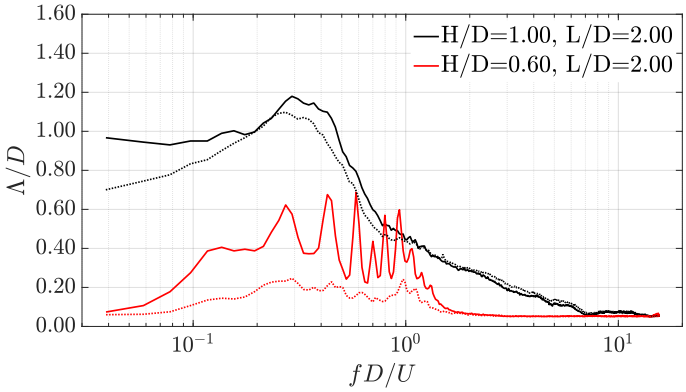

Figure 7: Surface TE span-wise correlation lengths [$H/D = 1, 0.6$, $L/D = 2$, $M_j = 0.6$].

case, the chevrons were seen to provide a slight (1.7dB) noise benefit at low and mid frequencies and a slight (1dB) penalty at high frequencies compared to the baseline round nozzle. This finding was consistent with the scientific literature. The differences between the two nozzles was even more apparent in the installed configuration. For very close wing-jet couplings, the chevrons significantly reduced both the broadband and the tonal noise components at low and mid frequencies. Analysis of the wall-pressure fluctuations, via two-point statistics, further demonstrated the ability of the chevrons to substantially reduce the span-wise coherence of the pressure field along the wing trailing edge. The authors suggest that the broadband behaviour is a consequence of the fact that chevrons generate stream-wise vorticity that suppresses the development of the Kelvin-Helmholtz instability in the jet shear layer. The tonal noise reduction is likely a consequence of the change in boundary condition in the jet that dictates whether a particular mode becomes trapped and is able to feedback between the nozzle lip and wing trailing edge. Finally, the span-wise surface TE correlation lengths were computed. The chevron jet was observed to halve this length-scale for the most aggressively coupled jet-wing configuration. The authors plan to use this knowledge to predict changes to the far-field noise using classic edge scattering theory.

ACKNOWLEDGEMENTS

The DJINN (Decrease Jet Installation Noise) project receives funding from the European Union's Horizon 2020 research and innovation programme under grant agreement No 861438. The DJINN project is a collaboration between CFDB (Coordinator), AIRBUS, DASSAULT, SAFRAN, RRD, ONERA, DLR, SOTON, CERFACS, ICL, VKI, CNRS, and QMUL.

REFERENCES

[1] C. Bogey C. Bailly and T. Castelain. Subsonic and supersonic jet mixing noise - chapter 1 in measurement, simulation and control of subsonic and supersonic jet noise. *VKI LS 2016-04, von Karman Institute for Fluid Dynamics*, 2016.

[2] B. Callender, E. Gutmark, and S. Martens. Far-field acoustic investigation into chevron nozzle mechanisms and trends. *AIAA journal*, 43(1):87–95, 2005.

[3] James Bridges and Clifford Brown. Parametric testing of chevrons on single flow hot jets. In *10th AIAA/CEAS aeroacoustics conference*, page 2824, 2004.

[4] Clifford Brown and James Bridges. Acoustic efficiency of azimuthal modes in jet noise using chevron nozzles. In *12th AIAA/CEAS Aeroacoustics Conference (27th AIAA Aeroacoustics Conference)*, page 2645.

[5] Steven Massey, Alaa Elmiligui, Craig Hunter, Russell Thomas, Paul Pao, and Vinod Mengle. Computational analysis of a chevron nozzle uniquely tailored for propulsion airframe aeroacoustics. 05 2006.

[6] Vinod Mengle, Ronen Elkoby, Leon Brusniak, and Russell Thomas. Reducing propulsion airframe aeroacoustic interactions with uniquely tailored chevrons: 1. isolated nozzles. In *12th AIAA/CEAS Aeroacoustics Conference (27th AIAA Aeroacoustics Conference)*, page 2467.

[7] Vinod Mengle, Ronen Elkoby, Leon Brusniak, and Russell Thomas. Reducing propulsion airframe aeroacoustic interactions with uniquely tailored chevrons: 2. installed nozzles. In *12th AIAA/CEAS Aeroacoustics Conference (27th AIAA Aeroacoustics Conference)*, page 2434.

[8] Vinod Mengle, Leon Brusniak, Ronen Elkoby, and Russell Thomas. Reducing propulsion airframe aeroacoustic interactions with uniquely tailored chevrons: 3. jet-flap interaction. In *12th AIAA/CEAS Aeroacoustics Conference (27th AIAA Aeroacoustics Conference)*, page 2435, 2006.

[9] Stefano Meloni, Jack LT Lawrence, Anderson R Proenca, Rod H Self, and Roberto Camussi. Wall pressure fluctuations induced by a single stream jet over a semi-finite plate. *International Journal of Aeroacoustics*, 19(3-5):240–253, 2020.

[10] Stefano Meloni, Matteo Mancinelli, Roberto Camussi, and Jerome Huber. *Wall pressure fluctuations induced by a compressible coaxial jet in installed configuration*. 2020.

[11] Stefano Meloni, Anderson R Proença, Jack LT Lawrence, and Roberto Camussi. An experimental investigation into model-scale installed jet–pylon–wing noise. *Journal of Fluid Mechanics*, 929, 2021.

[12] P. Welch. The use of fast fourier transform for the estimation of power spectra: A method based on time averaging over short, modified periodograms. *IEEE Transactions on Audio and Electroacoustics*, 15(2):70–73, 1967.

[13] H. E. Bass, L. C. Sutherland, A. J. Zuckerwar, D. T. Blackstock, and D. M. Hester. Atmospheric absorption of sound: Further developments. *The Journal of the Acoustical Society of America*, 97(1):680–683, 1995.

[14] H. E. Bass, L. C. Sutherland, A. J. Zuckerwar, D. T. Blackstock, and D. M. Hester. Erratum: Atmospheric absorption of sound: Further developments [j. acoust. soc. am. 97, 680–683 (1995)]. *The Journal of the Acoustical Society of America*, 99(2):1259–1259, 1996.

[15] Peter Jordan, Vincent Jaunet, Aaron Towne, André VG Cavalieri, Tim Colonius, Oliver Schmidt, and Anurag Agarwal. Jet–flap interaction tones. *Journal of Fluid Mechanics*, 853:333–358, 2018.